

# Kinematic study in FCCee CLD detector

*Report submitted by*

**Pradyot pritam sahu**

Roll No: 1811106

*supervised by*

**Dr. Prolay kumar mal**



*to the*

**School of Physical Sciences**

**National Institute of Science Education and Research**

**Bhubaneswar**

**November 27, 2022**

# Introduction

Based on the work for a detector at CLIC, this report provides a conceptual description and illustration of the CLD detector. CLD is one of the detectors planned for a future 100-kilometer  $e + e -$  linear circular collider (FCC-ee). The note also includes a brief description of the simulation and reconstruction tools used in the linear collider community, which have been adapted for physics and performance studies of CLD. We have learned about detector description which is an essential component to analyze data resulting from particle collisions in high energy physics experiments.

In this project, We have selected the *Higgs-Strahlung process* ( $e^+ + e^- \longrightarrow Z + H$ ) by  $e^+e^-$  collision at  $240\text{GeV}$  center of mass energy. We have run a fast parametric detector simulation with Delphes in the EDM4Hep format then applied event selection on those samples with FCCAnalyses and produced flat ntuples with observables of interest with FCCAnalyses. Then we have analyzed the different kinematics of *Higgs* and *Z* boson and their daughter particles with FCCAnalyses.

As we know *Z* boson is the exchange particles mediating weak interaction, which can decay when it produces. We have only focused on two of the detectable decay-modes, the decay into electron-positron ( $e^+e^-$ ) or muon-antimuon ( $\mu^+\mu^-$ ). We have studied different kinematic parameter such as energy ( $E$ ), transverse momentum ( $p_T$ ), momentum ( $p$ ), rapidity ( $y$ ),  $\theta$  of daughter particle and reconstructed its four momentum ( $p^\mu$ ). In order to satisfies invariant mass law we have reconstructed the mass of *Z* boson from their daughter particles.

# Description of CLD detectors<sup>[1]</sup>

## 2.1 Dimension and layout

In this following sections we have described the possible future CLD detector for FCC-ee [1]. This detector have a silicon pixel vertex detector and a silicon tracker, followed by highly granular calorimeters (a silicon-tungsten ECAL and a scintillator-steel HCAL). A superconducting solenoid provides a strong magnetic field, and a steel yoke interleaved with resistive plate (RPC) muon chambers closes the magnetic field. At this stage of the design of detector, it is assumed that the detector is identical for all the collision energies of FCC-ee, i.e. for operation at the  $Z(91.2\text{GeV})$ ,  $W(160\text{GeV})$ ,  $H(240\text{GeV})$  and  $top(365\text{GeV})$ .

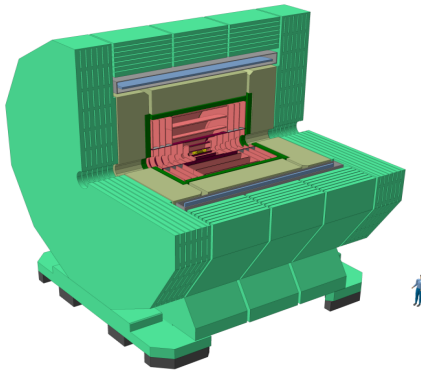


Figure 2.1: Isometric view of the CLD detector, with one quarter removed.

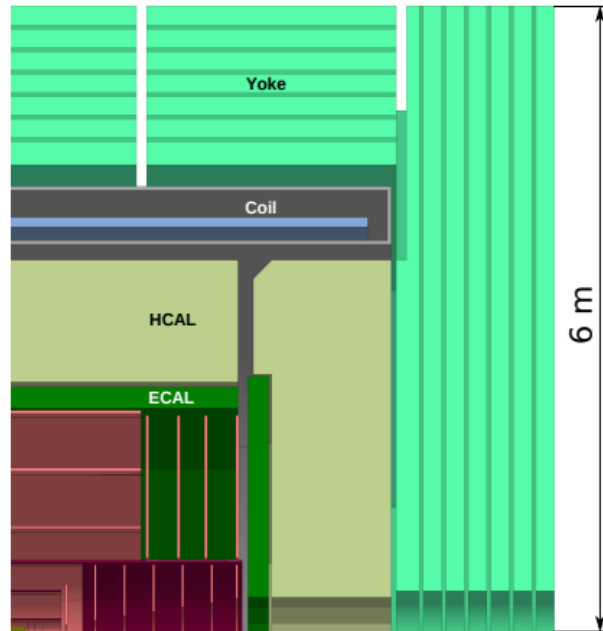


Figure 2.2: Vertical cross section showing the top right quadrant of CLD.

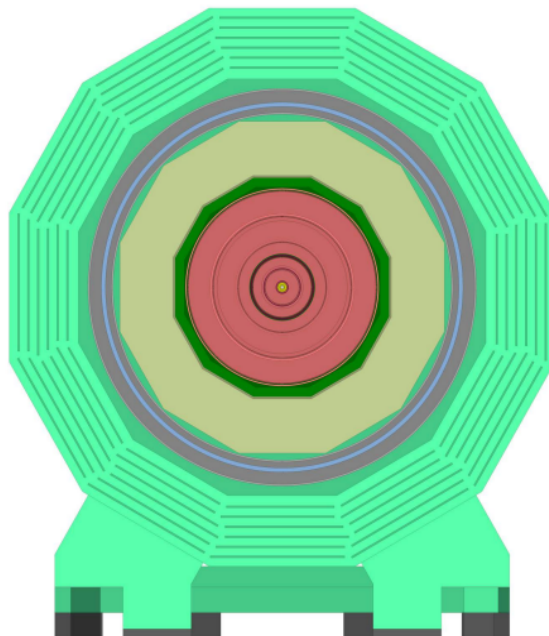


Figure 2.3: Transverse ( $XY$ ) cross section of CLD.

## 2.2 Vertex detector

The vertex detector in the CLD concept, a higher version of the one in CLICdet, consists of a cylindrical barrel detector closed off in the forward directions by discs. The layout is based on double layers, i.e. two sensitive layers fixed on a common support structure (which includes cooling circuits). The barrel consists of three double layers, the forward region is covered by three sets of double-discs on both sides of the barrel. An overview of the vertex detector layout is given in Figure(2.4). The total area of the vertex detector sensors is  $0.53m^2$ .

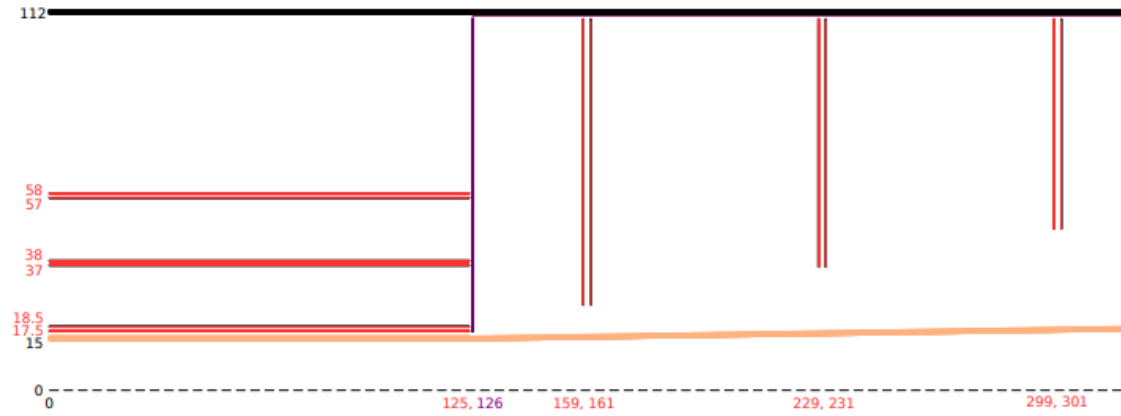


Figure 2.4: Vertex detector layout in ZR plane. Red lines indicating sensors, black lines indicating support structure and vacuum pipe in orange color.

The vertex detector consists of  $25 \times 25 \mu m^2$  pixels having a silicon sensor thickness of  $50 \mu m$ . Using pulse height information and charge sharing, a single point resolution of  $3 \mu m$  is aimed for. The overall length of the barrel vertex detector, built from staves, is 250 mm. The double layer structure is shown in Figure(2.5). The vertex detector forward region consists of three discs on each side where each disc is built as a double layer device. The discs are located a distance from the IP of 160, 230 and 300 mm respectively. They are constructed from 8 trapezoids, approximating a circle. For simplicity the trapezoids are not overlapping in the simulation model. The inner radii of the forward discs respect the 150 mrad cone reserved for MDI elements.

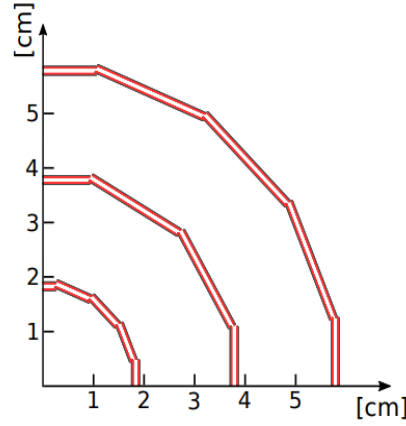


Figure 2.5: Vertex detector double layer structure in XY plane.

## 2.3 Silicon tracker

Like CLIC detector, the CLD concept have an all-silicon tracker. The inner tracker consists of three barrel layers and seven forward discs. The outer tracker has an additional three barrel layers and four discs. The overall layout of the silicon tracker in CLD is shown in Figure(2.6) . The tracking volume has a half-length of 2.2m

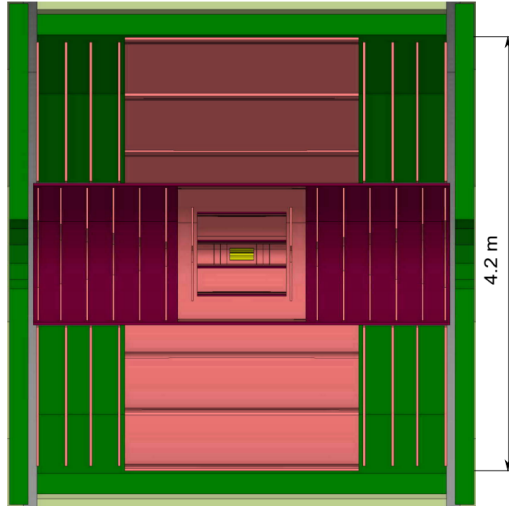


Figure 2.6: Overall layout of the CLD tracking system: the vertex barrel detector is shown in yellow, the tracking layers in lighter red. The surrounding ECAL is shown in green.

and a maximum radius of 2.1m. This radius allows to achieve a similar momentum resolution in the CLD tracking system with a 2T magnetic field as in the CLIC detector tracker with a 4T field and a radius of 1.5 m. The main support tube has an inner and outer radius of 0.686m and 0.690m respectively, and a half-length of 2.3 m. The tracking system covers polar angles larger than 150 mrad. The pixel vertex detector and the silicon tracker are treated as one unified tracking system in simulation and reconstruction.

## 2.4 Electromagnetic calorimeter(ECAL)

Further studies about ILC and CLIC have revealed that high granularity particle flow calorimetry appears to be a promising option to reach the required jet energy resolution of 3-4%. Such a performance is necessary to allow the distinction e.g. of  $W$  and  $Z$  bosons on an event-by-event basis. The segmentation of the ECAL has

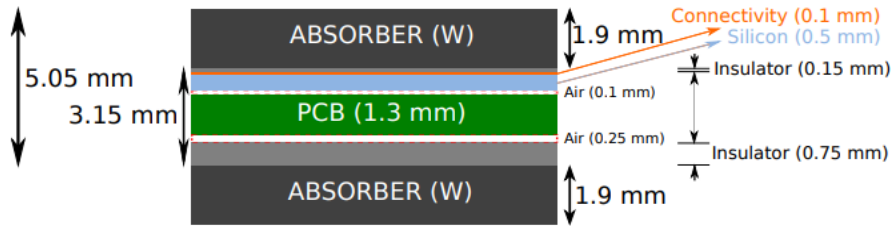


Figure 2.7: Schematic drawing of the ECAL segmentation as implemented in the simulation model

to be sufficient to resolve energy depositions from nearby particles in high energy jets. Studies performed in the context of the ILC and CLIC suggest a calorimeter transverse segmentation of  $5 \times 5 \text{ mm}^2$ . The technology chosen as baseline option for the detectors at the linear colliders is a silicon-tungsten sandwich structure as shown in Figure(2.7). This detector design is also implemented in the CLD simulation model.

## 2.5 Hadron calorimeter(HCAL)

The hadronic calorimeter of CLD has a structure and granularity as the one in CLICdet. It consists of steel absorber plates, each of them 19mm thick interleaved

with scintillator tiles. The gap for the sensitive layers and their cassette is 7.5mm. The polystyrene scintillator in the cassette is 3 mm thick with a tile size of  $30 \times 30$  mm<sup>2</sup>. In the simulations, the part of the HCAL endcap which surrounds the ECAL endcap is treated as a separate entity called the "HCAL ring". The detailed HCAL layer stack as implemented in the simulation model is shown in Figure(2.8).

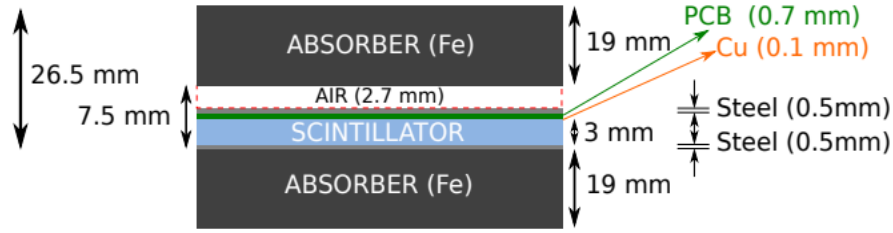


Figure 2.8: Schematic drawing of HCAL segmentation as implemented in the simulation model.

## 2.6 Magnet system

The solenoid magnetic field of the CLD detector is 2T, which is limited by MDI constraints. In the simulation model, the magnetic field in CLD is 2T throughout the volume inside the superconducting coil. The field in the yoke barrel is 1T, pointing in the opposite direction with respect to the inner field. The simulation model currently assumes no field in the yoke endcap nor outside the yoke.

## 2.7 Muon system

The iron yoke is divided into three rings in the barrel region and the two endcaps, as shown in Figure(2.9). The thickness of the yoke is reduced w.r.t. CLICdet, in correspondence to the lower solenoid field. A muon identification system with 6 layers as in CLICdet is implemented. An additional 7th layer is inserted in the barrel as close as possible to the coil. This layer may serve as tail catcher for hadron showers. The muon system layout in CLD is shown in Figure(2.10).



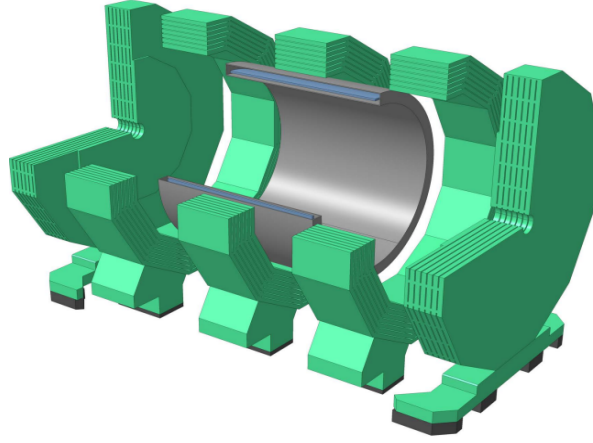


Figure 2.9: Segmentation of the iron return yoke of CLD into endcaps and three barrel rings.

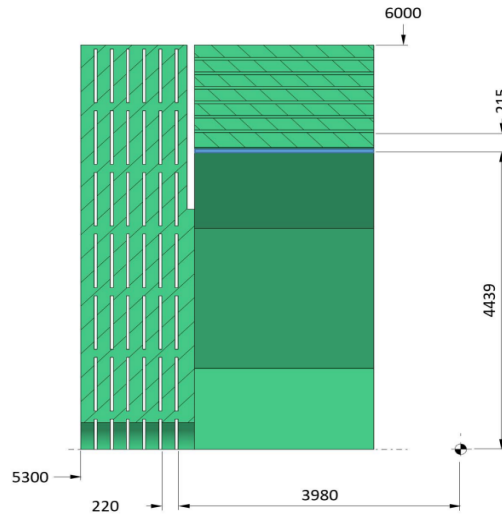


Figure 2.10: Schematic cross section of the muon system layout in the yoke of CLD.

## 2.8 FCCee: $e^+ + e^- \rightarrow Z + H$ process

### 2.8.1 Event generator - PYTHIA8

- To use Pythia8 we need a Gaudi steering file and a configuration file integrated in *Key4hep* software stack. The steering file is a python script that is used to configure the Gaudi framework which runs Pythia8. The configuration file is a text file that is used to configure the Pythia8 generator.
- In our case, data has been generated by selecting Higgs production (*HiggsSM* : *ffbar2HZ = on*) in collision of  $e^+$  (*Beams* : *idA = -11*) and  $e^-$  (*Beams* : *idB = 11*) collision at center of mass energy 240GeV. in pythia command file.

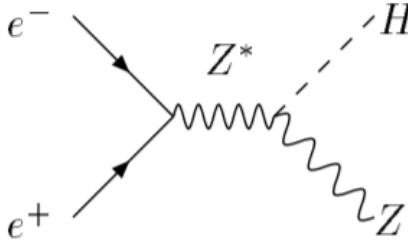


Figure 2.11: Higgs-strahlung process

- In this cases 100000 will be generated and saved in ROOT files in *EDM4hep* format. In order to get there we need first to generate the events in *HepMC* format.
- In order to get the events in *EDM4hep* format, we will use Gaudi and the tools available in *k4FWCore* and *k4Gen*. We need a Gaudi steering file that reads the *HepMC* file and writes out the *EDM4hep* file format for later processing in *DDSim*.

### 2.8.2 FCCee : Full simulation of CLD by DDSim

- We have set up the FCCSW software stack and used *DDSim* to simulate the detector response of CLD by `/cvmfs/sw - nightlies.hsf.org/key4hep/setup.sh`.
- The detectors in FCCSW are described in *DD4hep* compact files. The compact files are written in XML and expose configuration options for the detector.
- Then run the simulation with detector configuration file, event file and steering file and then run reconstruction.

### 2.8.3 Job submission in HTCondor batch system

The CERN Batch Service is a fairly standard High Throughput Computing (HTC) Batch System with a fair-sharing mechanism. Its purpose is to allow users to queue up jobs in the system, and maximise the utilisation of the batch farm.

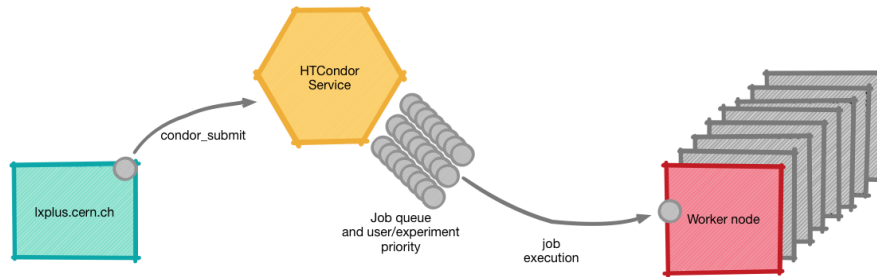


Figure 2.12: HTCondor

Here we have submit our job to the batch system. The job is discrete and independent of other jobs. The job is submitted to the batch system and the batch system will run the job and return the output to the user. The batch system will also keep track of the jobs and their status.

- HTCondor provides the ability to match executables files using regular expressions and add a job to the queue for each file.
- In our case we have queued 10 jobs for respective `.sh` executable file. The 10 jobs, even if they have different executables, have the same Cluster and different ProcIds.

#### **2.8.4 Analysis of Delphes samples**<sup>[2]</sup>

We have used Delphes sample to get the detector response of CLD. Delphes is a fast detector simulation framework. It is based on the fast simulation package FastJet and uses the ROOT data analysis framework. The FCCAnalyses framework is based on the RDataFrame interface which allows fast and efficient analysis of ROOT's TTrees and on samples following the *EDM4HEP* event data model. Here we have produced flat ntuples with observables of interest and then produced plots with FCCAnalyses.

# Result and Discussion

## 3.1 $Z \longrightarrow \mu^+ + \mu^-$ process

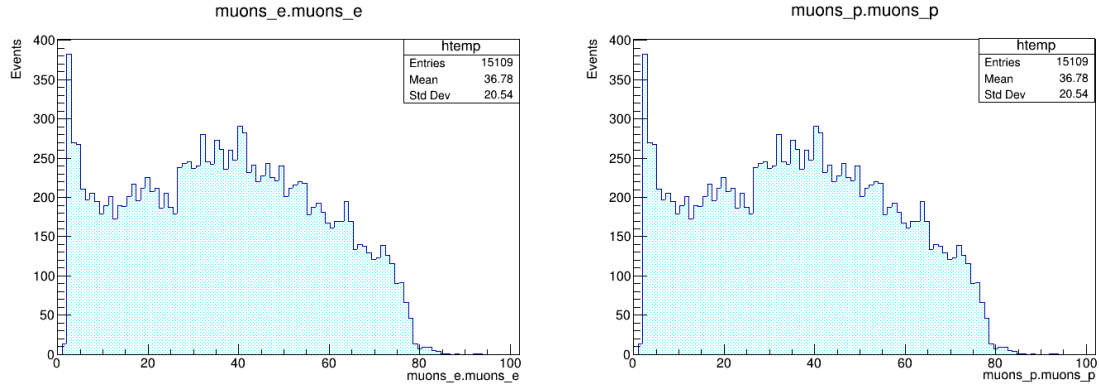


Figure 3.1: Energy and momentum distribution of  $\mu^+$  and  $\mu^-$  at 240 GeV.

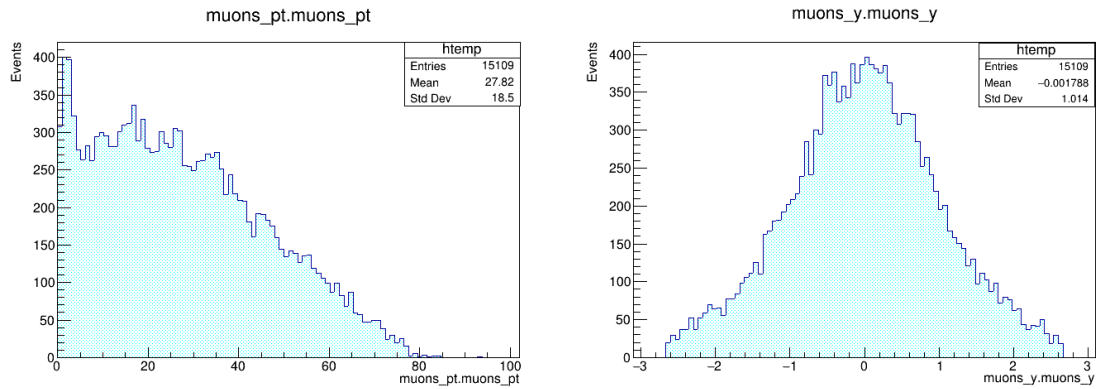


Figure 3.2: Transverse momentum and rapidity distribution of  $\mu^+$  and  $\mu^-$  at 240 GeV.

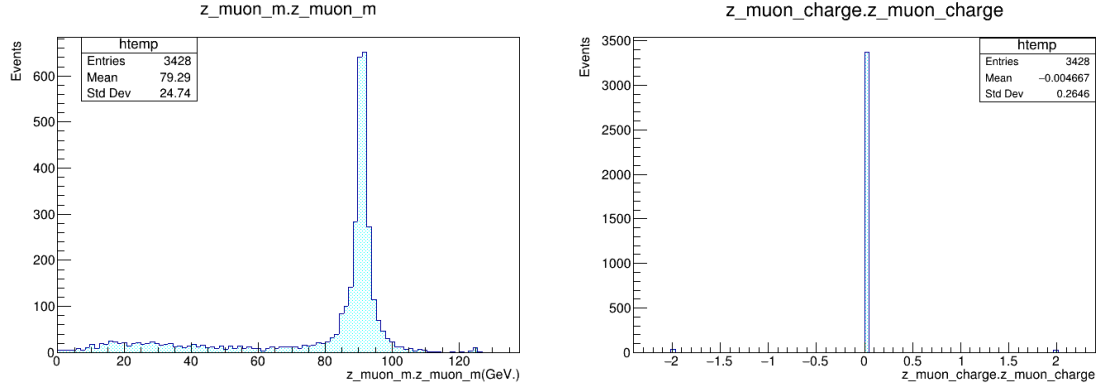


Figure 3.3: Reconstructed mass and charge from  $\mu^+$  and  $\mu^-$  at 240GeV.

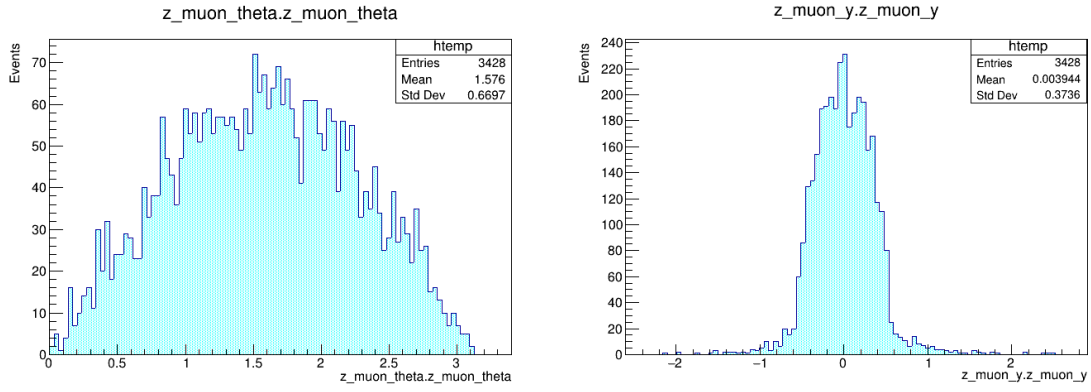


Figure 3.4: Reconstructed  $\theta$  and rapidity from  $\mu^+$  and  $\mu^-$  at 240GeV.

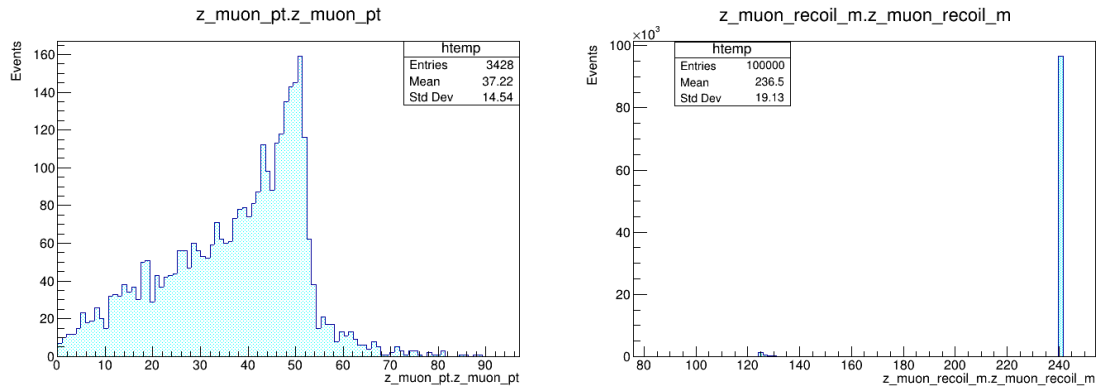


Figure 3.5: Reconstructed transverse momentum and recoil mass from  $\mu^+$  and  $\mu^-$  at 240GeV.

### 3.2 $Z \longrightarrow e^+ + e^-$ process

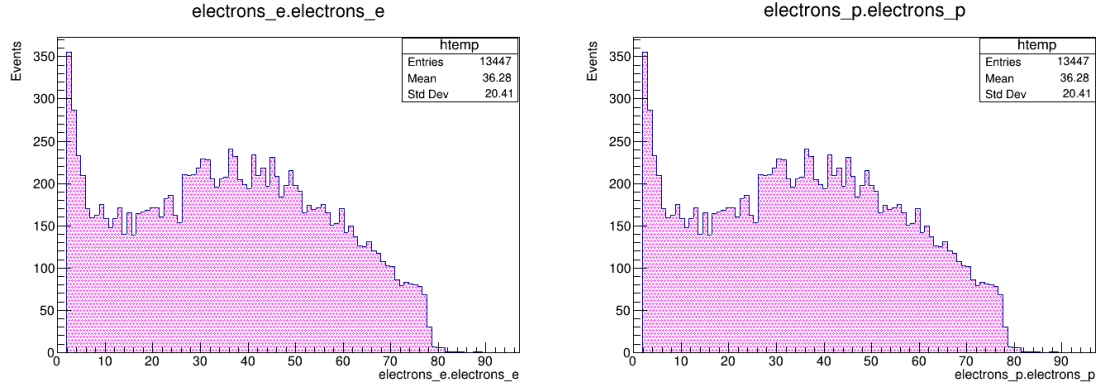


Figure 3.6: Energy and momentum distribution of  $e^+$  and  $e^-$  at 240GeV.

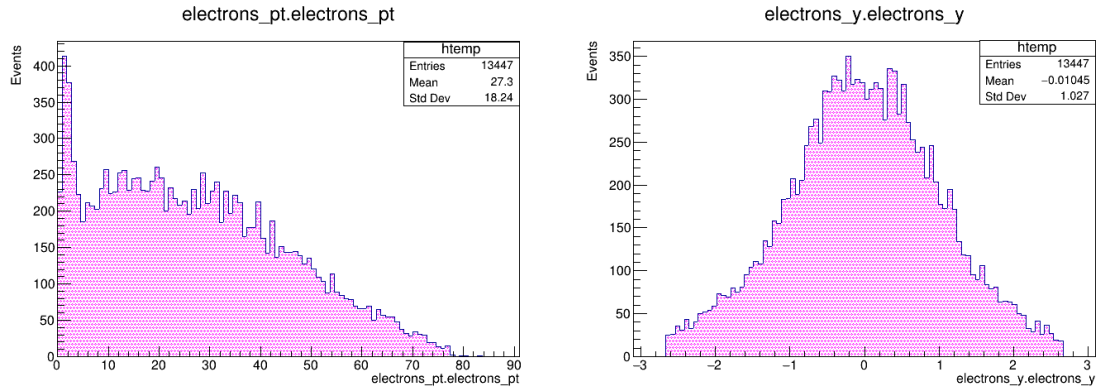


Figure 3.7: Transverse momentum and rapidity distribution of  $e^+$  and  $e^-$  at 240GeV.

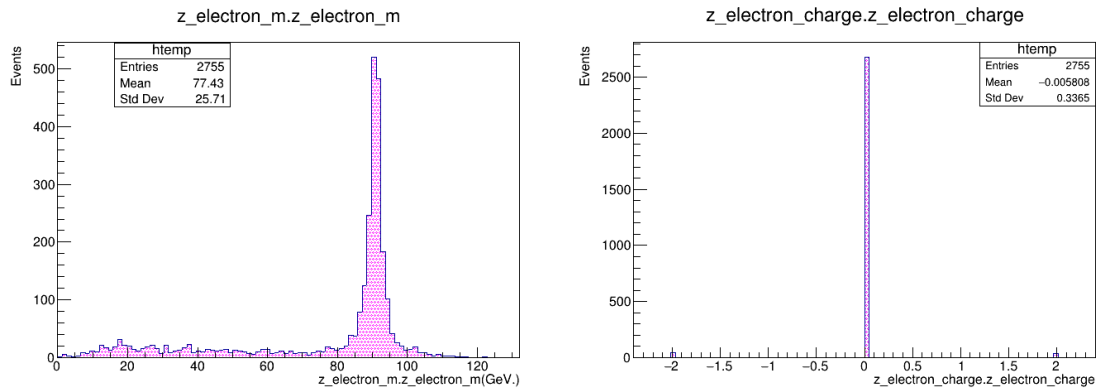


Figure 3.8: Reconstructed mass and charge from  $e^+$  and  $e^-$  at 240GeV.

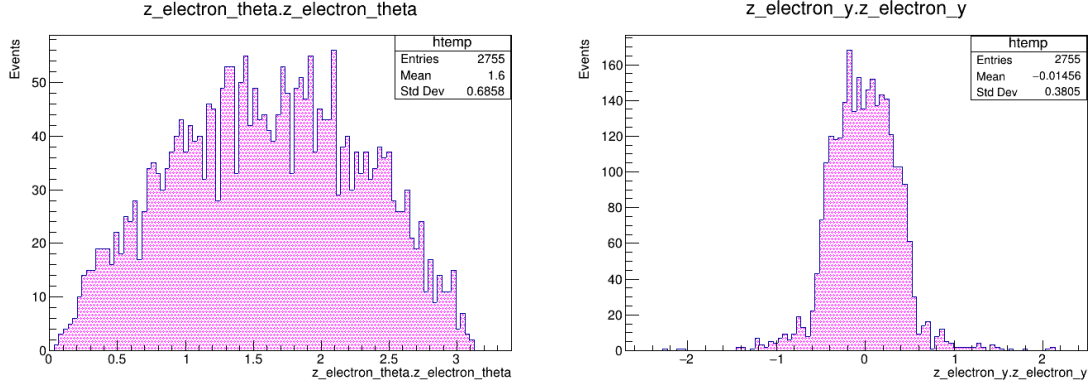


Figure 3.9: Reconstructed  $\theta$  and rapidity from  $e^+$  and  $e^-$  at 240GeV.

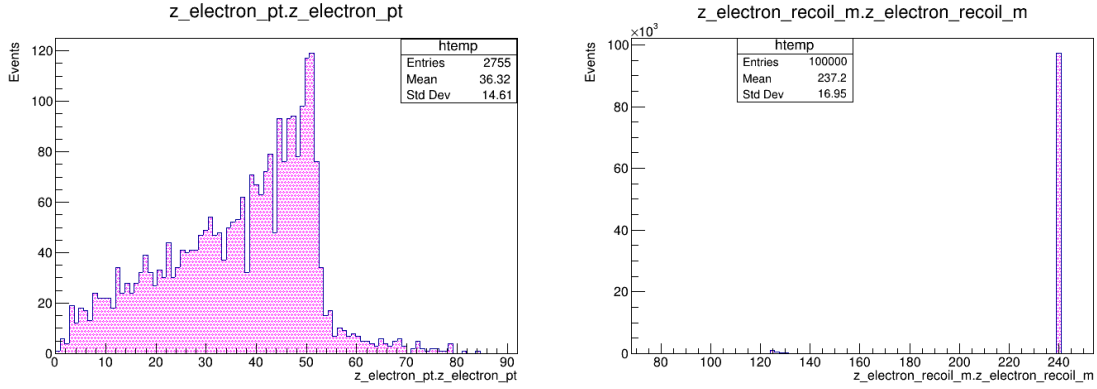


Figure 3.10: Reconstructed transverse momentum and recoil mass from  $e^+$  and  $e^-$  at 240GeV.

From figure(3.3) and (3.8) we have got the distributions of the reconstructed Z mass for  $Z \rightarrow \mu^+ + \mu^-$  and  $Z \rightarrow e^+ + e^-$  respectively. A peak can be seen around 91GeV. in both distributions, which matches the Z boson mass.



# Conclusion

We have reconstructed the mass of  $Z$  boson from  $e^+e^-$ ,  $\mu^+\mu^-$  in decay of  $Z$  which satisfies invariant mass law and also studied different kinematic parameter as shown in previous section. The analysis performed by running a fast parametric detector simulation with Delphes in the EDM4Hep format. Then we have applied an event selection on our delphes sample with FCCAnalyses and produced flat ntuples with observables of interest with FCCAnalyses. By analysing the ntuple produced with ROOT's RDataFrame and used the ROOT's TTree class to store the data in a tree structure and then used the ROOT's TCanvas class to plot the data in a graph format.

# Future study

We will generate the signal with background samples and apply fast parametric detector simulation with Delphes in the EDM4Hep format, then analysis it as we have done in this project. We will also study the different kinematics of Higgs boson and its daughter particles. Later we will study the tracking efficiency and jet energy resolution of the detector.

# References

- [1] The CLD Detector Concept- [https://indico.cern.ch/event/1064327/contributions/4893180/attachments/2452299/4204992/220601\\_FCCWeek\\_CLD\\_sailer.pdf](https://indico.cern.ch/event/1064327/contributions/4893180/attachments/2452299/4204992/220601_FCCWeek_CLD_sailer.pdf)
- [2] <https://github.com/HEP-FCC/FCCeePhysicsPerformance/blob/master/General/README.md#How-to-associate-RecoParticles-with-Monte-Carlo-Particles>
- [3] <https://hep-fcc.github.io/fcc-tutorials/fast-sim-and-analysis/FccFastSimGeneration.html>
- [4] Bacchetta, N., et al. "CLD – A Detector Concept for the FCC-ee." arXiv, 2019, <https://doi.org/10.48550/arXiv.1911.12230>. Accessed 25 Nov. 2022.